materials proceedings

Proceeding Paper

Characterization of Siderophores Produced by *Glutamicibacter* sp. Strain AlTeq-24-F2

Ángel Martínez-Arreola, Gabriela Martínez-Mejía, Jair Cruz Narváez, Lazaro Ruiz-Virgen, Rubén Caro-Briones, Belem Chávez-Ramírez and Mónica Corea-Téllez

MDPI

https://doi.org/10.3390/materproc2025025015

materials proceedings

MDPI

Proceeding Paper

Characterization of Siderophores Produced by *Glutamicibacter* sp. Strain AlTeq-24-F2 †

Ángel Martínez-Arreola [1], Gabriela Martínez-Mejía [1,*], Jair Cruz Narváez [1], Lazaro Ruiz-Virgen [1], Rubén Caro-Briones [2], Belem Chávez-Ramírez [3] and Mónica Corea-Téllez [1]

[1] Laboratorio de Investigación de Polímeros y Nanomateriales, Escuela Superior de Ingeniería Química e Industrias Extractivas, Instituto Politécnico Nacional, México City 07738, Mexico; angel000309@gmail.com (Á.M.-A.); ycruzn@ipn.mx (J.C.N.); lazaro1990@hotmail.com (L.R.-V.); mcorea@ipn.mx (M.C.-T.)
[2] Escuela Superior de Ingeniería Mecánica y Eléctrica, Instituto Politécnico Nacional, México City 07738, Mexico; rcaro@ipn.mx
[3] Laboratorio de Fitopatología, Escuela Nacional de Ciencias Biológicas, Instituto Politécnico Nacional, México City 07700, Mexico; belcha0615@gmail.com
* Correspondence: gamartinezm@ipn.mx
† Presented at the 5th International Online Conference on Nanomaterials, 22–24 September 2025; Available online: https://sciforum.net/event/IOCN2025.

Abstract

Siderophores are low-molecular-weight chelating agents secreted by microorganisms under iron-limiting conditions, playing a crucial role in metal bioavailability and microbial survival. In this study, siderophores produced by *Glutamicibacter* sp. strain Al-Teq-24-F2, isolated from plant-associated samples, were characterized through a combination of spectroscopic and analytical methods. ESI-MS analysis of the crude extract revealed several abundant ions between 175 and 800 m/z, suggesting a mixture of secondary metabolites. After chromatographic purification, FT-IR and NMR analyses indicated the presence of amide, hydroxyl, and carboxylate functional groups. Integrating these data allowed for the proposal of a siderophore structure with a molecular weight of 438.25 Da. Thermogravimetric analysis showed thermal stability below 115 °C. During Fe (III) complexation, the zeta potential shifted from −21.15 mV to +42 mV, confirming strong interaction between the ligand and the metal. UV–Vis and fluorescence spectroscopy displayed characteristic bathochromic and hypochromic shifts, together with pronounced fluorescence quenching upon iron binding. These findings provide new insight into the structural and physicochemical properties of siderophores produced by *Glutamicibacter* sp. and highlight their potential applications in biosensing and metal chelation processes.

Keywords: *Glutamicibacter*; siderophore; iron chelation; FT-IR; NMR; ESI-MS; metabolomics

Academic Editor: Jose L. Arias Mediano

Published: 15 December 2025

Citation: Martínez-Arreola, Á.; Martínez-Mejía, G.; Narváez, J.C.; Ruiz-Virgen, L.; Caro-Briones, R.; Chávez-Ramírez, B.; Corea-Téllez, M. Characterization of Siderophores Produced by *Glutamicibacter* sp. Strain AlTeq-24-F2. *Mater. Proc.* **2025**, *25*, 15. https://doi.org/10.3390/materproc2025025015

1. Introduction

Iron is an essential micronutrient for almost all living organisms and plays critical roles in respiration, DNA synthesis, and redox enzymatic reactions. However, under aerobic and neutral pH conditions, ferric iron (Fe^{3+}) is poorly soluble, with concentrations often below 10^{-6} M insufficient to sustain microbial growth. To overcome this limitation, microorganisms evolved low-molecular-weight chelators known as siderophores. These compounds solubilize iron and transport it into the cell through specific uptake systems. These compounds are produced by bacteria, fungi, and plants under iron-limiting envi-

ronments and exhibit remarkable structural diversity that determines their metal-binding properties and ecological functions [1–3].

Siderophores are typically grouped into catecholates, hydroxamates, and carboxylates. Hydroxamates usually contain ornithine derivatives, while carboxylate-type ligands are common in non-ribosomal peptides. In bacteria of the genus Pseudomonas, siderophores such as pyroverdins and pyrochelins containing hydroxamate groups have been extensively studied as models of metal acquisition and fluorescence-based signaling [4–6]. In contrast, *Glutamicibacter* species remain poorly studied in terms of siderophore production and structure. Although Arthrobacter species are known to produce hydroxamate-type siderophores (e.g., artrobactin), little is known about the chemical nature or coordination behavior of their *Glutamicibacter* counterparts [7–9].

Beyond their biological role, siderophores have gained interest for several biotechnological applications, such as heavy metal bioremediation, plant growth promotion through improved iron acquisition, and the development of biosensors and antimicrobial conjugates. In medicine, synthetic analogs such as deferoxamine B are clinically employed for iron and aluminum detoxification. Moreover, siderophore–antibiotic conjugates, known as "Trojan horse" systems, represent a promising strategy to overcome antibiotic resistance by exploiting bacterial iron uptake pathways [10–13].

Given their multifunctionality, the discovery and structural elucidation of new siderophores can expand the chemical space of bioactive metal chelators and provide insight into microbial adaptation in metal-stressed environments. The characterization of siderophores from novel or poorly described genera is thus a relevant step toward understanding microbial diversity and harnessing these metabolites for sustainable applications [14,15].

The present work focuses on the physicochemical characterization of siderophores produced by *Glutamicibacter* sp. AlTeq-24-F2, combining spectroscopic, chromatographic, and analytical techniques to elucidate their structural and functional properties [16,17].

The present work focuses on the physicochemical characterization of siderophores produced by *Glutamicibacter* sp. AlTeq-24-F2, combining spectroscopic, chromatographic, and analytical techniques to elucidate their structural and functional properties [16,17]. The supernatant was purified by chromatography and analyzed by FT-IR, Raman, ESI-MS, and NMR. Thermal stability and chelation capacity were also assessed through thermogravimetric and zeta potential analyses. Additional analyses, including thermogravimetric and zeta potential measurements, were conducted to evaluate the stability and chelation capacity of the purified compounds toward Fe^{3+} ions. The integration of these techniques allowed the proposal of a chemical structure containing a carboxylate-type ligand with a molecular weight of approximately 438 Da. Moreover, spectroscopic evidence confirmed the formation of a stable Fe(III)–siderophore complex, as indicated by characteristic shifts in UV–Vis and fluorescence spectra.

This research contributes new information to the limited knowledge of siderophore production by *Glutamicibacter* species and provides a foundation for future studies on their biosynthetic pathways, ecological roles, and potential applications in biotechnology and materials science.

2. Materials and Methods

2.1. Materials

Bacterial supernatants from *Pseudomonas* sp. strain AlTeq-24-F1 and *Glutamicibater* sp. strain AlTeq-24-F2 were provided by the Phytopathology Laboratory at the National School of Biological Sciences (ENCB-IPN, Mexico). The minimal King B medium was used as the culture medium. Analytical-grade solvents, methanol and ethyl acetate (Negociaciones

D'Mik, San Isidro, Mexico), silica gel 60 F_{254} (Merck, Darmstadt, Germany), and deionized water (Barnstead MicroPure purification system, Thermo Scientific, Waltham, MA, USA) were used. Deuterated methanol (CD_3OD, 99 atom % D, Sigma-Aldrich, Burlington, MA, USA) was employed for NMR analyses. Ferric chloride hexahydrate ($FeCl_3 \cdot 6H_2O$, Fermont, Monterrey, Mexico) was used for complexation assays.

2.2. Bacterial Culture

To prepare the bacterial suspension required for this study, we followed the standard procedure: the bacteria were cultured in King B medium, which contains peptone, glycerol, and K_2HPO_4 as its main components and is widely used to promote siderophore production in fluorescent and non-fluorescent bacteria. The medium was prepared according to standard formulations and sterilized at 121 °C for 15 min prior to inoculation. For cultivation, each strain was inoculated into 250 mL Erlenmeyer flasks containing 100 mL of sterile King B medium and incubated at 28 °C with shaking at 150 rpm for 48 h. These conditions were selected to favor the secretion of extracellular metabolites in iron-limited environments. After incubation, the cultures were centrifuged for 15 min, and the cell-free supernatant was collected for further analysis.

2.3. Chromatographic Separation

A preliminary thin-layer chromatography (TLC) screening was used to determine the optimal mobile phase (ethyl acetate/methanol, 1:1 v/v). Column chromatography was performed using packed silica gel in a 1 cm diameter burette. The dried supernatant was extracted with the same solvent mixture, and the eluates (1–2 mL fractions) were collected and monitored by TLC under UV light (254 nm) and $KMnO_4$ staining. Fractions with similar Rf values were pooled and concentrated for further analysis.

2.4. Gravimetric Analysis

The total solid content of the supernatants was determined gravimetrically. Aluminum crucibles were weighed, filled with 0.1–0.5 mL of sample, dried at 60 °C for 48 h, and reweighed. The solid fraction (%) was calculated as the ratio of dry residue mass to the initial solution mass [18].

2.5. Infrared Spectroscopic Characterization

FT-IR spectra were recorded using a Perkin Elmer 1605 (Waltham, MA, USA) spectrophotometer equipped with an ATR accessory (650–4000 cm^{-1}). Raman spectra were obtained with a Horiba Jobin Yvon LabRam HR800 (Kyoto, Japan) spectrometer using a 785 nm laser. UV–Vis spectra were measured on a Perkin Elmer Lambda 25 spectrophotometer (200–700 nm) (Waltham, MA, USA). Fluorescence emission was recorded on a Shimadzu RF-6000 fluorometer (Kyoto, Japan) at 230 nm excitation and 250–500 nm emission range.

2.6. Mass Spectrometry and Metabolomic Profiling

Samples were analyzed by ESI-TOF mass spectrometry (Bruker micrOTOF, Germany) in positive-ion mode (50–3000 m/z). High-resolution metabolomic analysis was performed using a Solarix XR 7T FT-ICR-MS (Bruker Daltonics, Germany). Detected ions were compared with the Natural Products Atlas database for tentative metabolite identification.

2.7. Nuclear Magnetic Resonance (NMR)

^1H, ^{13}C, and HSQC spectra were acquired at 500 MHz and 200 MHz, respectively, on a Bruker Avance III spectrometer. Approximately 150 mg of each purified fraction was dissolved in CD_3OD. Chemical shifts were referenced to residual solvent peaks at δ = 4.87 ppm (^1H) and δ = 49 ppm (^{13}C).

2.8. Iron Chelation and Zeta Potential Measurements

Solutions of purified fractions (15 g L^{-1}) were titrated with $FeCl_3 \cdot 6H_2O$ (12.5 mM for Pseudomonas and 14.8 mM for *Glutamicibacter* siderophores). Zeta potential (ζ) and pH were measured using a Malvern Zetasizer Nano ZSP (Malvern, UK) equipped with an automatic titration unit. Measurements were performed in quadruplicate at 25 °C to determine the isoelectric point and complex stability.

3. Results

3.1. Gravimetric Analysis

The dry supernatant values are shown as a function of the initial supernatant mass in Figure 1. The data obtained were adjusted using linear regression, resulting in a solids rate of 2.04%p for SoGlu. This behavior showed a consistent linear relationship between the initial mass of the supernatant and the solid remaining after drying, which supports the stability and reproducibility of the total solids calculation. The rate obtained of 2.04%p allows us to infer that the culture generates a moderate amount of biomass and extracellular metabolites, sufficient for the subsequent purification and characterization of siderophores. Converting this value to biomass equivalent units, a concentration of 19.2 g/L was estimated, which is significantly higher than that reported in the literature for bacterial systems cultured in King B medium, such as Pseudomonas fluorescens (≈2 g/L) [19]. This difference suggests that *Glutamicibacter* AlTeq-24-F2 has remarkable metabolic efficiency under conditions of low iron availability, which is consistent with its edaphic origin and adaptation to resource-limited environments [2].

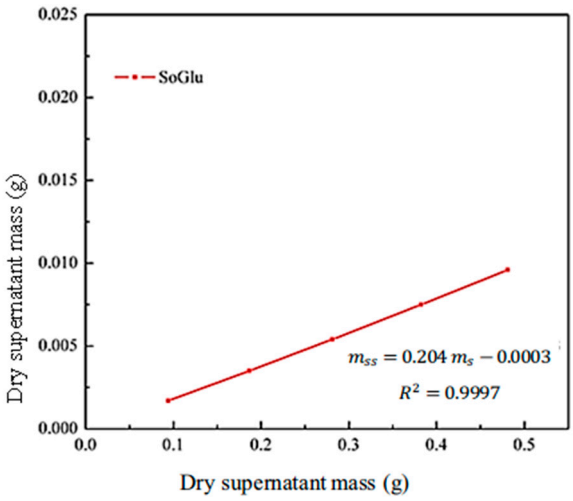

Figure 1. Gravimetry of the supernatants.

3.2. Infrared Spectroscopic Characterization

The spectra obtained from SoGlu are shown in Figure 2, where transmittance bands at 3305 cm^{-1} corresponding to the vibration of the NH bond in amides can be observed, although their overlap with signals attributable to O–H groups from the aqueous medium is also possible. A signal at 1635 cm^{-1} corresponds to the carbonyl C=O vibration of amides, a common spectroscopic signature in non-ribosomal peptides and carboxylate-type siderophores [20]. These signals suggest the presence of peptide or protein compounds, possibly related to metabolites secreted during bacterial growth [21].

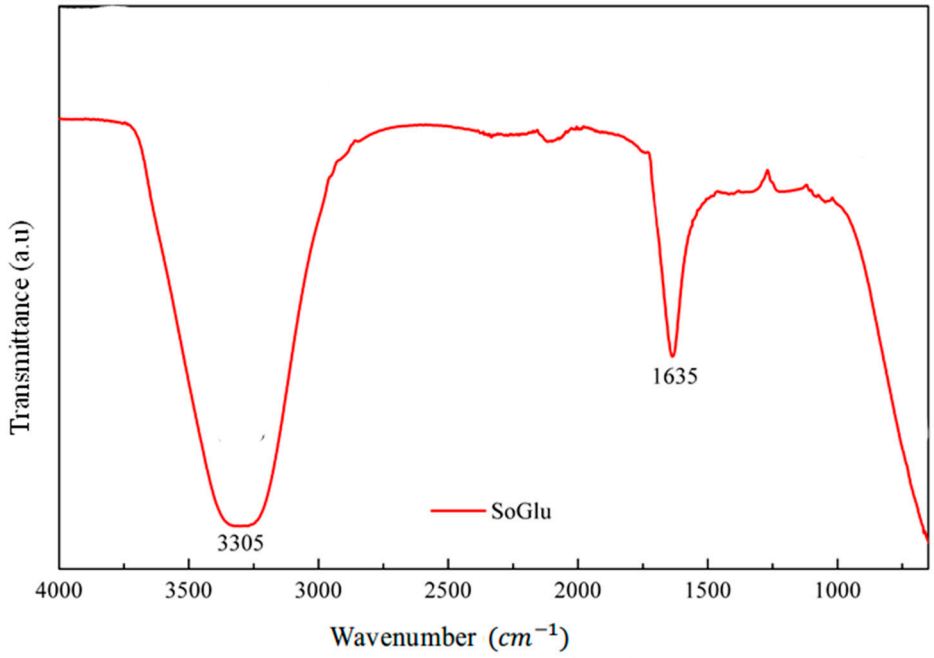

Figure 2. FT-IR spectra of the supernatants.

3.3. Mass Spectrometry and Metabolomic Profiling

The mass spectrum of the SoGlu supernatant (Figure 3) shows signals at 175.1174, 381.297, 648.2672, and 800.3336 m/z. Although the signals presented usually correspond in microbial metabolomics to fragments of organic acids or monoaromatic/hydroxyalkyl units that may derive from the partial degradation of peptides or siderophore subunits [22], complementary experimentation is necessary in order to provide a reliable structural assignment.

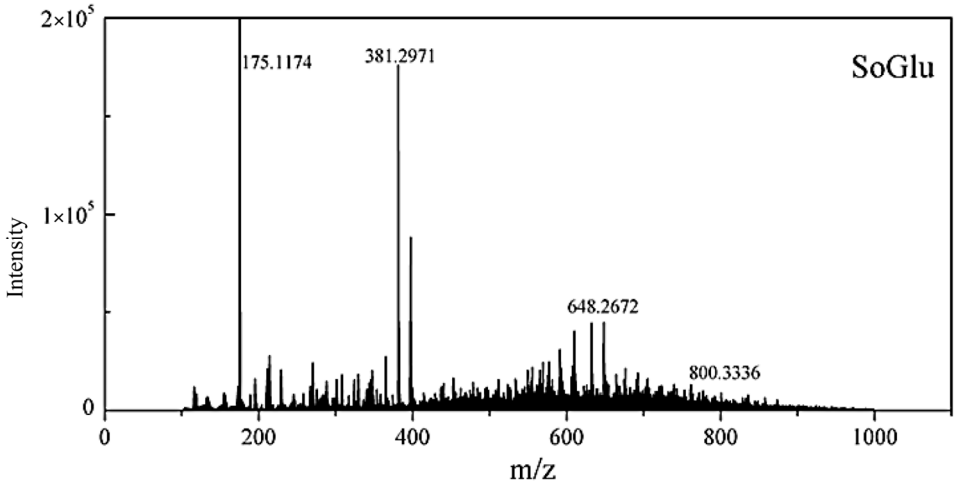

Figure 3. ESI-MS spectrum of negative ions of SoGlu.

The supernatants were analyzed in a Fourier transform ion cyclotron resonance mass spectrometer for metabolomic analysis. This technique uses the mass-to-charge (m/z) values of the adducts. The values obtained are compared with metabolite databases to provide an approximation of the metabolites that the supernatant may contain [17]. Using the Natural Products Atlas database, the mass spectra were processed and filtered, reducing the dataset to 7412 signals. Of these, 250 ions matched known compounds, forming 33 molecular networks, each containing between 2 to 53 compounds, and their distribution is shown in Figure 4. This organization indicates that the bacterium produces

structurally coherent sets derived from common biosynthetic pathways, probably linked to the synthesis of siderophores and their variants. The presence of large, well-defined clusters suggests that there is a dominant metabolomic pathway in the supernatant, which is consistent with the ESI-MS and FT-IR results and supports the existence of a major siderophore accompanied by minor structural derivatives [23].

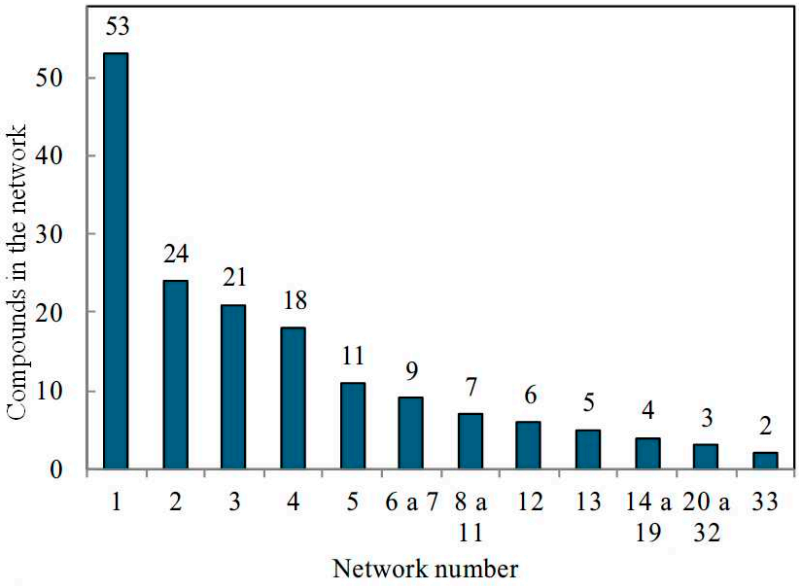

Figure 4. Networks with compounds identified in SoGlu.

3.4. Nuclear Magnetic Resonance (NMR)

The spectra obtained from 1D NMR spectroscopy for the SidGlu fraction are shown in Figure 5, and the 2D spectrum is shown in Figure 6.

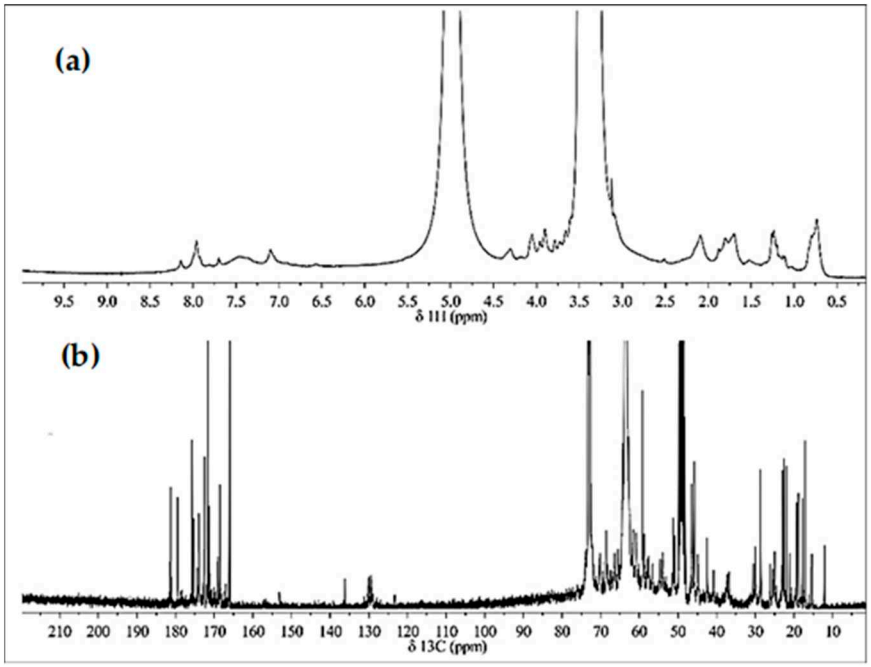

Figure 5. (**a**) ^{1}H and (**b**) ^{13}C NMR spectra of SidGlu.

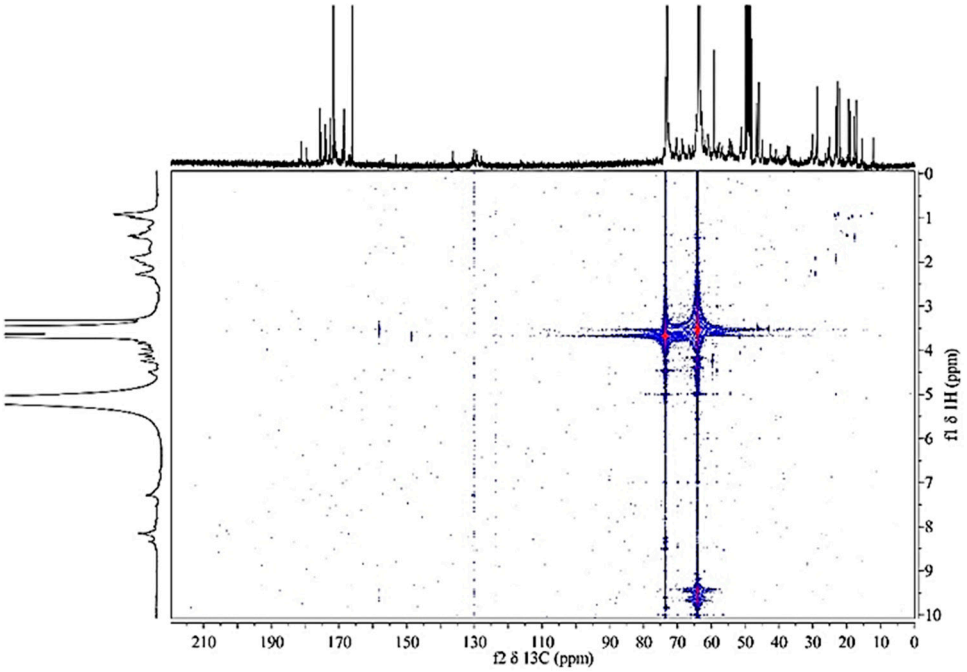

Figure 6. HSQC NMR spectrum of SidGlu.

In Figure 5a, the chemical shifts of ^{1}H correspond to δ protons [ppm]: 0.75–2.0 for alkanes (*RCH_n-R*, *n* = 1, 2, 3) and alkyl ketone (*RCH$_n$C (=O)R*, *n* = 1, 2, 3); 2.5–3.1 for amines (*RCH$_n$NR$_2$* or *RCH$_n$NH$_2$*, *n* = 1, 2, 3); 3.2–4.0 for alcohols (*RCH$_n$OH*, *n* = 1, 2); 4.75–5.5 for alkenes (*RCH$_n$ = CHR* or *RCH$_n$ = CHR$_2$*, *n* = 1, 2); and 6.5–8.5 for aromatics (*H-Ar*) [23]. Similarly to the previous case, a broadening of the signals is observed, which prevents the multiplicity of the proton signals from being obtained. The chemical shifts obtained by ^{13}C NMR are shown in Figure 5b, and the carbons observed are in δ [ppm]: 10–25 (*R-CH$_3$*), 18–50 (*R-CH$_2$-R*), and 20–60 (*R$_3$-CH*) for alkanes; 20–55 for amines (*RCH$_n$NR$_2$* or *RCH$_n$NH$_2$*, *n* = 1, 2, 3); 42–75 for alcohols (*R-CH$_n$-OH*, *n* = 1, 2); 120–140 for alkenes (*RCH$_n$ = CR$_2$*, *n* = 1, 2) and aromatics (*C-Ar*); and 150–185 for amides (*RC(=O)ONR$_2$*) and carboxylic acids (*RC(=O)OH*) [23].

The proposed structure was obtained by combining the functional groups identified in the 1D NMR spectra and comparing them with the HSQC correlation spectrum in Figure 6, which correlates protons with the carbon atoms to which they are directly bonded [24]. The proposed structure is shown in Figure 7; it has a molecular weight of 438.25 Da and a condensed formula of $C_{26}H_{34}N_2$. It has carbonyl and amide domains consistent with the signals detected in FT-IR and with the ions observed in ESI-MS. The absence of aromatic patterns and the predominance of functionalized aliphatic shifts suggest a carboxylate-type siderophore with a relatively compact architecture, capable of forming stable complexes with Fe(III). Taken together, the NMR data corroborate the identity of the major metabolite as a modified peptide siderophore, whose proposed structure is consistent with both the exact mass detected and the spectroscopic behavior observed in the various analytical techniques.

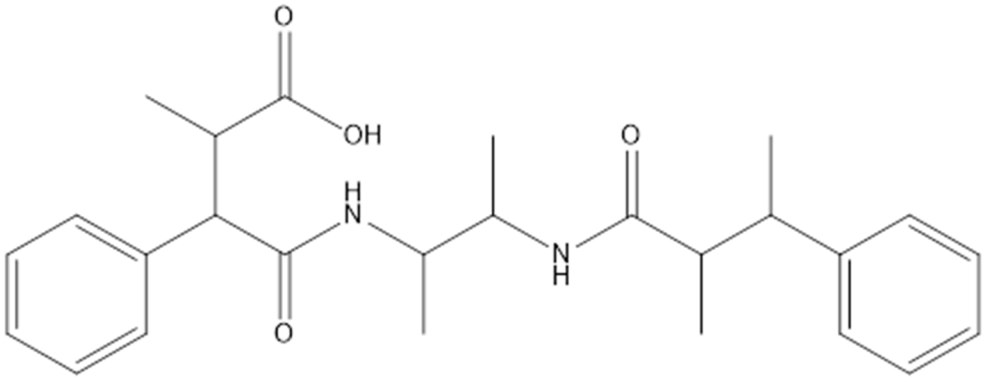

Figure 7. Proposed structure for the siderophore of *Glutamicibacter* sp. key AlTeq 24 F2.

3.5. Iron Chelation and Zeta Potential Measurements

The solutions prepared with the fractions were evaluated for their ability to chelate with iron. To do this, the solutions were titrated with a $FeCl_3 \cdot 6H_2O$ solution with a concentration of 14.8 mM for SiGlu; during each injection, potential ζ and pH values were measured. The results are shown in Figure 8. For SidGlu, the initial solution shows a ζ potential value of −21.15 mV, indicating that the system is stable and that the negative surface charge is due to the carbonyl groups present in the molecule [25]. When the ferric chloride solution is added, the ζ potential changes to positive values, indicating the interaction of the siderophore present in the fraction and the iron. The isoelectric point occurred at 0.59 mM ferric chloride, and the final potential value of 42 mV indicates high stability of the complex in the solution [26]. Similarly, the pH changes from an initial value of 4.21 to 3.53, indicating deprotonation and the formation of hydrochloric acid. These results demonstrate that the major molecule detected in SoGlu not only possesses the functional groups necessary to coordinate iron (as indicated by FT-IR and NMR) but also forms kinetically and thermodynamically favored complexes with Fe(III) in solution. This supports its classification as an active siderophore and suggests potential applications in metal remediation or sensing, where the formation of soluble and stable complexes is a key requirement. To complete the characterization, additional MS/MS titration experiments of the complex and stability studies against variations in ionic strength and pH would confirm the stoichiometry and robustness of the complex under more diverse environmental conditions [24].

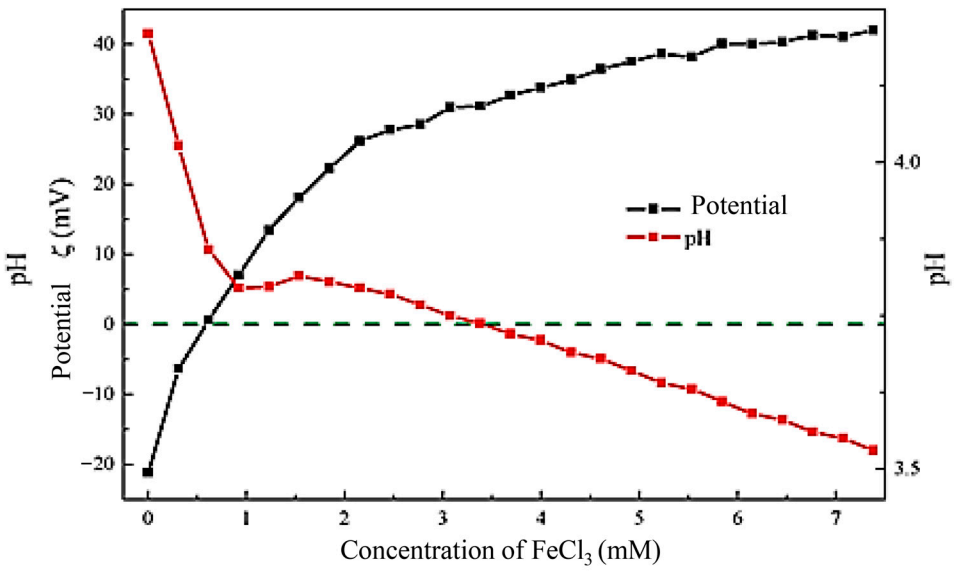

Figure 8. Graphs of potential ζ and pH as a function of ferric chloride concentration.

Although this work integrates multiple analytical techniques for the characterization of the siderophore produced by *Glutamicibacter* sp. AlTeq-24-F2, some limitations remain. The structural elucidation is partial and would benefit from targeted MS/MS fragmentation and additional NMR experiments to confirm the proposed architecture. Moreover, further assays are required to define the chelation stoichiometry and to evaluate the behavior of the siderophore under different environmental conditions.

Despite these limitations, the study provides a significant contribution by identifying a carboxylate-type siderophore in a genus historically underexplored for siderophore production. The integration of FT-IR, MS, FT-ICR-MS, NMR, and zeta potential analyses offers robust multi-level evidence of its structure and function, positioning *Glutamicibacter* AlTeq-24-F2 as a promising candidate for biotechnological applications related to iron mobilization and metal chelation.

4. Conclusions

Glutamicibacter sp. AlTeq-24-F2 produced a carboxylate-type siderophore confirmed by amide and carbonyl signals in FT-IR.

The marked change in zeta potential during titration with Fe(III) confirmed the formation of stable iron–ligand complexes.

The siderophore from *Glutamicibacter* sp. AlTeq-24-F2 shows promising physicochemical properties, particularly in fluorescence and metal binding. These features suggest it has potential for applications in metal sensing or bioremediation.

Author Contributions: Conceptualization, M.C.-T.; methodology, G.M.-M.; software, Á.M.-A.; validation, J.C.N.; formal analysis, G.M.-M.; investigation, Á.M.-A. and R.C.-B.; resources, M.C.-T. and B.C.-R.; data curation, L.R.-V.; writing—original draft preparation, M.C.-T. and B.C.-R.; writing—review and editing, G.M.-M.; visualization, G.M.-M.; supervision, M.C.-T.; project administration, M.C.-T.; funding acquisition, M.C.-T. and B.C.-R. All authors have read and agreed to the published version of the manuscript.

Funding: This research received no external funding.

Institutional Review Board Statement: Not applicable.

Informed Consent Statement: Not applicable.

Data Availability Statement: The data supporting the findings of this study are not publicly available due to institutional restrictions.

Acknowledgments: We acknowledge the Centro de Nanociencias y Micro y Nanotecnología for the analyses using mass spectrometry and nuclear magnetic resonance techniques.

Conflicts of Interest: The authors declare no conflict of interest.

References

1. Butler, A.; Theisen, R.M. Iron(III)–siderophore coordination chemistry: Reactivity of marine siderophores. *Coord. Chem. Rev.* **2010**, *254*, 288–296. [CrossRef] [PubMed]
2. Hider, R.C.; Kong, X. Chemistry and biology of siderophores. *Nat. Prod. Rep.* **2010**, *27*, 637–657. [CrossRef]
3. Neilands, J.B. Siderophores: Structure and function of microbial iron transport compounds. *J. Biol. Chem.* **1995**, *270*, 26723–26726. [CrossRef]
4. Budzikiewicz, H. Siderophores of the *Pseudomonadaceae sensu* stricto (Fluorescent and Non-Fluorescent *Pseudomonas* spp.). In *Progress in the Chemistry of Organic Natural Products*; Herz, W., Falk, H., Kirby, G.W., Eds.; Springer: New York, NY, USA, 2004; Volume 87, pp. 81–237. [CrossRef]
5. Meyer, J.M.; Abdallah, M.A. The fluorescent pigment of Pseudomonas fluorescens: Biosynthesis, purification and physicochemical properties. *Microbiology* **1978**, *107*, 319–328. [CrossRef]
6. Cornelis, P.; Matthijs, S. Diversity of siderophores in fluorescent Pseudomonads: Not only pyoverdines. *Environ. Microbiol.* **2002**, *4*, 797–808. [CrossRef]

7. Busse, H.-J. Review of the taxonomy of the genus Arthrobacter and proposal to reclassify selected species as *Glutamicibacter* gen. nov. *Int. J. Syst. Evol. Microbiol.* **2016**, *66*, 9–37. [CrossRef] [PubMed]
8. Winkelmann, G. Specificity of iron transport in bacteria and fungi. In *CRC Handbook of Microbial Iron Chelates*; CRC Press: Boca Raton, FL, USA, 1991; pp. 65–104. [CrossRef]
9. Cleary, J.L.; Kolachina, S.; Wolfe, B.E.; Sanchez, L.M. Coproporphyrin III produced by the bacterium Glutamicibacter arilaitensis binds zinc and is upregulated by fungi in cheese rinds. *mSystems* **2018**, *3*, e00036-18. [CrossRef] [PubMed]
10. Kong, H.; Cheng, W.; Wei, H.; Yuan, Y.; Yang, Z.; Zhang, X. An overview of recent progress in siderophore–antibiotic conjugates. *Eur. J. Med. Chem.* **2019**, *182*, 111615. [CrossRef]
11. Deb, C.; Tatung, M. Siderophore-producing bacteria as biocontrol agents against phytopathogens for a better environment: A review. *S. Afr. J. Bot.* **2024**, *164*, 48–62. [CrossRef]
12. Zulkernain, N.; Uvarajan, T.; Chuan, C. Roles and significance of chelating agents for potentially toxic elements (PTEs) phytoremediation in soil: A review. *J. Environ. Manag.* **2023**, *346*, 117926. [CrossRef]
13. Soares, E.V. Perspective on the biotechnological production of bacterial siderophores and their use. *Appl. Microbiol. Biotechnol.* **2022**, *106*, 5407–5424. [CrossRef]
14. Carroll, C.S.; Moore, M.M. Ironing out siderophore biosynthesis: A review of NRPS-independent siderophore synthetases. *Crit. Rev. Biochem. Mol. Biol.* **2018**, *53*, 356–381. [CrossRef]
15. Challis, G.L.; Naismith, J.H. Structural aspects of non-ribosomal peptide biosynthesis. *Curr. Opin. Struct. Biol.* **2004**, *14*, 748–756. [CrossRef]
16. Meyer, J.M.; Geoffroy, V.A.; Baida, N.; Gardan, L.; Izard, D.; Lemanceau, P.; Achouak, W.; Palleroni, N.J. Siderophore typing, a powerful tool for the identification of fluorescent and nonfluorescent Pseudomonads. *Appl. Environ. Microbiol.* **2002**, *68*, 2745–2753. [CrossRef]
17. Morehouse, N.; Clark, T.N.; McMann, E.; van Santen, J.A.; Linington, R.G. Annotation of natural product compound families using molecular networking topology and structural similarity fingerprinting. *Nat. Commun.* **2023**, *14*, 276. [CrossRef] [PubMed]
18. Santillán, R.; Nieves, E.; Alejandre, C.P.; Gómez-Yañez, C.; del Río, J.M.; Dorantes-Rosales, H.; Navarro-Clemente, M.E.; Corea, M. Synthesis of highly carboxylated latex particles using a power feed process. *J. Ind. Eng. Chem.* **2013**, *19*, 1257–1266. [CrossRef]
19. Vindeirinho, J.M.; Soares, H.M.V.M.; Soares, E.V. Modulation of siderophore production by *Pseudomonas fluorescens* through the manipulation of the culture medium composition. *Appl. Biochem. Biotechnol.* **2021**, *193*, 607–618. [CrossRef] [PubMed]
20. Mistry, B. *Handbook of Spectroscopy Data Chemistry (UV, IR, PMR, 13CNMR and Mass Spectroscopy)*; Oxford Book Company: Oxford, UK, 2009; ISBN 978-81-89473-86-0.
21. Kamnev, A.; Dyatlova, Y.; Kenzhegulov, O.; Fedonenko, Y.; Evstigneeva, S.; Tugarova, A. Fourier Transform Infrared (FTIR) Spectroscopic Study of Biofilms Formed by the Rhizobacterium *Azospirillum baldaniorum* Sp245: Aspects of Methodology and Matrix Composition. *Molecules* **2023**, *28*, 1949. [CrossRef]
22. Hiserodt, R.; Brown, S.; Switjer, D.; Hawkins, N.; Mussian, C. A study of b1+H_2O and b1-Ions in the Product Ion Spectra of Dipeptides Containing N-Terminal Basic Amino Acid Residues. *J. Am. Soc. Mass Spectrom.* **2007**, *18*, 1414–1422. [CrossRef] [PubMed]
23. Natural Products Atlas (Sin Fecha) (Base de datos versión 2024_09). Available online: https://www.npatlas.org/ (accessed on 10 November 2025).
24. Field, L.; Li, H.; Magill, A. *Organic Structures from 2D NMR Spectra*; Wiley: Hoboken, NJ, USA, 2015; ISBN 13: 978-1118868942.
25. Bhattacharjee, S. DLS and zeta potential—What they are and what they are not? *J. Control. Release* **2016**, *235*, 337–351. [CrossRef]
26. Ruiz-Virgen, L.; Hernandez-Martinez, M.; Martínez-Mejía, G.; Caro-Briones, R.; Herbert-Pucheta, E.; Río, J.; Corea, M. Analysis of Structural Changes of pH–ThermoResponsive Nanoparticles in Polymeric Hydrogels. *Gels* **2024**, *10*, 541. [CrossRef] [PubMed]